16th ICAAR LISBOA 2020-2022

16th International Conference on
Alkali-Aggregate Reaction in Concrete
Lisboa | LNEC | Portugal | 31 May - 2 June 2022

http://icaar2020-2022.lnec.pt

Effect of confinement on steel-concrete bond behavior of alkali-silica reactive (ASR) concrete

Olesya Zhychkovska [(1)], Shamim A. Sheikh [(2)], Daman K. Panesar [(3)]

(1) University of Toronto, Toronto, Canada, olesya.zhychkovska@mail.utoronto.ca

(2) University of Toronto, Toronto, Canada, sheikh@ecf.utoronto.ca

(3) University of Toronto, Toronto, Canada, d.panesar@utoronto.ca

Abstract

Bond behaviour of steel bars embedded in the alkali-silica reactive (ASR) concrete was examined and compared to that in the control (REG) concrete. Pull-out bond cylinder specimens (36 made with reactive and 36 control concrete) were tested under direct tension to study bond. Test variables included the type of concrete, longitudinal and transverse reinforcements and extent of ASR damage. Testing of both unconfined and confined pull-out specimens was conducted at three different concrete ages (23, 132 and 212 days since the onset of curing) to observe the effect of different levels of concrete deterioration on bond performance. All the specimens were subjected to the accelerated curing conditions (50 ± 2°C and 97±3% RH) to promote ASR over a 7-month period. Evolution of ASR concrete mechanical properties during this time was also investigated using dozens of specimens.

Test results showed that ASR concrete compressive strength increased over time, albeit at a slower rate than for the nonreactive concrete. While compressive strength of the reactive concrete increased by 51% over its 28-day value, stiffness dropped by 19%. The unconfined reactive specimens exhibited a 20% loss in the pull-out bond strength, while in the reinforced cylinders no reduction in bond strength was observed. However, at later stages of ASR deterioration the normalized bond capacity of the control concrete was generally greater than that of the reactive concrete.

Keywords: *alkali-silica reaction; bond-slip response; bond strength; confinement; material properties*

1. INTRODUCTION

Alkali-silica reaction (ASR) is a chemical process resulting from the interaction between the reactive siliceous minerals contained in some aggregates and alkali supplied by cement paste. Reaction by-product, known as the alkali-silica gel, induces tensile stresses within the affected concrete medium, leading to concrete cracking and subsequent degradation.

Since reaction's first discovery by Stanton [1] in the 1930s, sources of alkali-silica reactive aggregates have been located all over the world. Over the years countries like United Kingdom, Denmark, Canada, Japan, U.S.A. among others, have encountered and reported large-scale components of infrastructure, including bridges, dams and nuclear power plants, deteriorating from ASR [2]. While present design and construction strategies aim at identifying and eradicating the deleterious aggregates from usage in concrete production [3], concerns are being raised about the load-carrying capacity of the existing structures suffering from ASR.

Vast majority of experimental work on ASR affected concrete has been dedicated to the material behaviour of plain un-reinforced concrete [4–7], as well as to the response of reinforced elements under flexure and shear [8–14]. Despite the worldwide attention to the issues triggered by the alkali-silica reactivity, studies on bond behaviour of concrete suffering from ASR are scarce. Risks associated with the impacts of ASR on bond are twofold. Bond characteristics can be affected directly by the products of the reaction, or indirectly, through concrete cover cracking and ingress of the chemically aggressive agents, leading to steel corrosion.

One of the most comprehensive studies on bond between steel and ASR concrete was performed by Chana [15] which involved pull-out testing of 16 mm diameter bars to investigate the effects of bar type (plain or ribbed), casting position (top vs. bottom), cover concrete thickness, and presence of transverse reinforcement on bond characteristics. Specimens were cured inside the water conditioning tanks at 20°C for 28 days after casting with the subsequent temperature increase to 38 °C until extensive

cracking was observed in the reactive prisms. At the time of testing unrestrained expansion of reactive concrete was around 0.4%.

Bond strength of the ribbed bars decreased by as much as 40% due to ASR in concrete with no transverse reinforcement and was similar to the reduction in concrete tensile strength. On the other hand, 13% and 24% of bond strength was lost in the bottom and top cast bars, respectively, when transverse reinforcement was provided. These results were also in good agreement with the data presented by Clark from the Konoike Construction Co. Ltd. [16].

Haddad and Numayr [17] investigated bond between 18 mm deformed steel bars and ASR concrete in the unconfined concrete cylinders using two types of reactive aggregates (Mix A and B). Testing was conducted at three distinct phases depending on the severity of concrete cracking due to ASR. The pre-cracking, cracking and post-cracking stages were identified. Specimens were conditioned for two months in 0.5 NaOH water at 40 °C.

Despite the higher percentage of reactive aggregates and lower compressive strength of mix B, the final unrestrained expansion of both mixes was within the same range (0.29% vs 0.31% for mix B and A, respectively). However, peak bond stresses developed in specimens cast from mix B concrete were consistenly lower than those determined in cylinders made from mix A. Bond strength of mix B was continuously dropping as the amount of longitudinal expansion was rising, albeit at a lower rate than the critical bond stress. Critical bond stress, defined as the stress at the slip onset, decreased in both mixes as the level of damage due to ASR increased. On the other hand, a significant level of concrete expansion had to be reached prior to any degradation of bond strength and bond stiffness in mix A. Overall, bond strength reduction of 11% and 24% was observed in mixes A and B, respectively, at the final post-cracking stage compared to the pre-cracking results.

2. EXPERIMENTAL PROGRAM

Experimental investigation presented here included a total of 72 pull-out specimens with various type of reinforcement and two different concrete mix designs. However, due to the space limitations current paper solely focuses on the results from the pull-out tests conducted on 36 specimens with no reinforcement (NR group), and the ones containing reinforcement cages made of longitudinal bar and transverse spirals (TRLN group). Discussion of bond behavior of specimens with only the longitudinal bars (LN group) or spirals (TR group) can be found elsewhere [18].

2.1 Materials

2.1.1 Concrete mix proportions

Two concrete mixes were prepared for the current experimental work with the only main variable being the degree of reactivity of the coarse aggregates. Control mix (REG) contained nonreactive limestone in the coarse fraction with the expansive potential of 0.015% as determined from the standardized ASTM C1293 [19] test. Reactive mix (ASR), on the other hand, incorporated the alkali-silica susceptible Spratt aggregate with the expansion potential of 0.202% as measured following the same guidelines. To accelerate alkali-silica reaction and achieve higher expansion, the mix proportions used for the ASR concrete were as follows: 23.3% for aggregates between 19.0- and 12.5-mm size fraction; 33.3% for 12.5-9.5 mm and 43.3% for 9.5-4.75 mm, adopting the recommendations made by Gautam [20] who observed up to 50% more expansion compared to the mixture containing the conventional equal proportions of the three sizes of coarse aggregate following ASTM C1293 [19].

In additon, fine constituents comprised of the nonreactive sand. Its reactive potential of 0.032% was determined in accordance with ASTM C1260 [21], and was much lower than the prescribed limit of 0.10%. Other physical characteristics of both coarse and fine aggregates are summarized in Table 2.1.

Water-cement ratio of both mixes was 0.51 to attain good concrete workability. Total alkali content of the General use (GU) Portland cement as reported by the manufacturer was 0.92% Na_2O equivalent by mass of cement. The desirable alkalinity of the reactive concrete mix was 1.25% Na_2O_{eq} to accelerate the chemical processes between the reactive siliceous components of Spratt aggregates and alkali from cement paste. To achive this cement alkali level sodium hydroxide pellets (NaOH) were added to the mixing water of reactive concrete. Concrete mix designs for both REG and ASR specimens are summarized in Table 2.2. Because of the limited capacity of the mixer, four concrete batches were prepared, two for control specimens and two for reactive.

Table 2.1: Physical properties of fine and coarse aggregates

Aggregate Type	Reactivity	Dry-rodded density, kg/m^3	Relative Density, kg/m^3	Water Absorption, %
Coarse	Nonreactive	1579	2685	1.48
	Reactive (Spratt)	1596	2666	0.58
Fine	Nonreactive		2741	0.67

Table 2.2: Concrete mix designs

Material	Control Concrete (REG)	Reactive Concrete (ASR)
Cement, kg/m^3	420	420
Water, kg/m^3	214.2	214.2
Coarse Aggregates, kg/m^3	1105.2*	1116.9*
Sand, kg/m^3	650.2	630.6
Added Alkali Pellets, kg/m^3	0	1.79

*Difference in the quantities of coarse aggregates is due to the variation of aggregates dry-rodded densities

2.1.2 Steel reinforcement

All the specimens were reinforced concentrically with a single 20M reinforcing bar (Grade 400W). Bar rib height and spacing were 1.34 mm and 11.6 mm, respectively. Additionally, cylinder specimens from the TRLN group were reinforced with the steel cages made of transverse #3 US spirals and 10M longitudinal bars. Mechanical properties of steel are listed in Table 2.3.

Table 2.3: Reinforcing steel material properties

Rebar Designation	Nominal Diameter, mm	Nominal Area, mm^2	Elastic Modulus, GPa	Yield Strength, MPa	Yield Strain, $\times10^{-3}$	Onset of strain hardening, $\times10^{-3}$	Tensile Strength, MPa	Ultimate strain, $\times10^{-3}$
#3	9.5	71	182	438	2.47	15.4	662	134.1
10M	11.3	100	202	434	2.15	14.9	611	169.5
20M	19.5	300	193	433	2.21	14.7	591	140.1

2.2 Test specimens

Cylindrical specimens were 165 mm in diameter and 300 mm high. Conventional pull-out specimen configuration was utilized, with one 1-m long 20M bar protruding concentrically from the cylinder. Reinforcement was bonded to concrete over a distance equal to $5Ø_b$ (i.e. 100 mm) as shown in Figure 2.1(a).

Nine REG and nine ASR specimens had no reinforcement (NR group), while the remaining 18 cylinders were reinforced with the spirals and longitudinal bars (TRLN group). The longitudinal reinforcement ratio was 1.4% of the gross specimen area and the spiral reinforcement was 2.18% of the core area with the core diameter (D_c) of 130 mm measured to the outside of the spiral. Drawings of the specimens' geometry and reinforcement are provided in Figure 2.1(b) and (c).

Additionally, several companion specimens were cast together with the pull-out specimens to determine concrete compressive strength, Young's modulus and free expansion. These included twelve 100 mm diameter and 200 mm long cylinders and three 75 × 75 × 285 mm expansion prisms produced from each concrete batch. All the companion specimens were subjected to the same storage conditions before and after their placement inside the environmental chamber as the pull-out specimens.

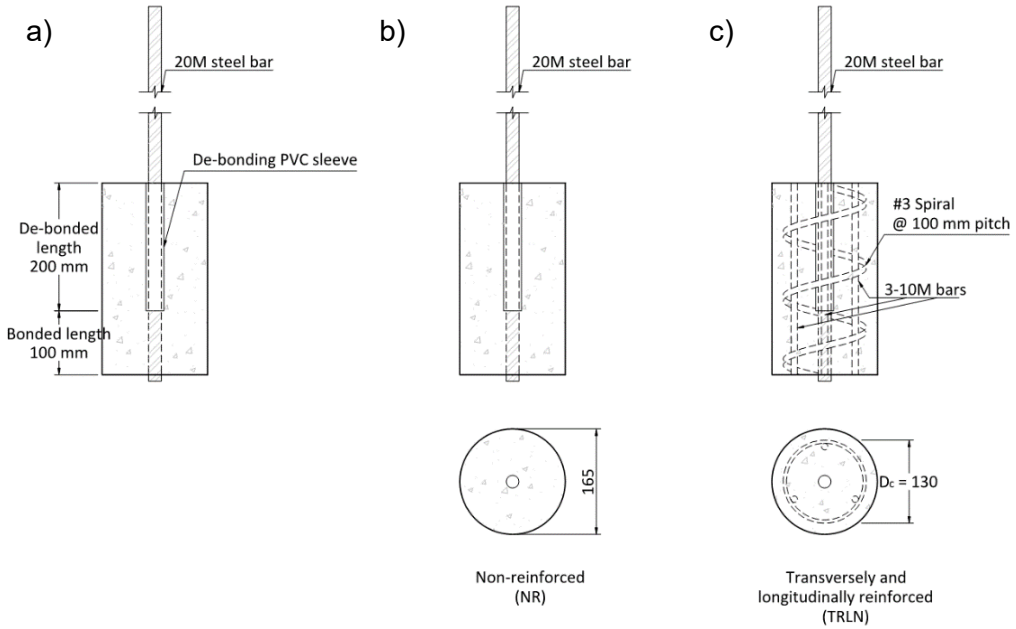

Figure 2.1: a) Details of pull-out test specimens with the b) NR and c) TRLN configurations

2.3 Specimen conditioning regime

All the specimens were demolded 24 hours after casting, and continuously wet cured for the following 6 days. After one week of curing all the specimens were allowed to mature at the ambient lab conditions (~25°C and ~65% RH) until their placement inside a curing facility to promote ASR.

To accelerate the evolution of the alkali-silica reaction, the pull-out and auxiliary specimens were subjected to the high humidity and temperature environment inside a well-insulated conditioning facility constructed at the University of Toronto. Conditions inside the environmental chamber were constantly maintained at around 50 ± 2°C and 97 ± 3% RH by means of heating fans and steam distribution unit mounted inside the curing room. Specimens made with both reactive and control concrete were placed inside the chamber at the same time to facilitate the direct comparison in their behaviour during testing. At the onset of conditioning REG pull-out and companion specimens were around 379 days old, while ASR were about 344 days of age due to the delays caused by the complications encountered in the construction and operation of the chamber.

2.4 Pull-out tests

Pull-out tests were carried out after 23, 132 and 212 days of accelerated curing (labelled as test Phase 0, 1 and 2). Three identical REG and ASR replicates were tested at the same time corresponding to each test age. Companion specimens were also tested alonside the pull-out cylinders to determine concrete material properties at the time of testing.

Pull-out tests were performed using the 1,000-kN capacity Universal Testing Machine. Figure 2.2(a) and (b) provide details of the experimental setup in both schematic and pictorial formats, respectively. Rigid steel frame, consisting of two horizontal plates connected with 4 hollow steel posts, was used to apply the load to the cylinder surface. Machine was operated in the displacement-controlled mode with the initial loading rate of 0.010 mm/sec, which was gradually increased to 0.030 mm/sec in the post-peak slip range.

Loaded end bar displacement relative to the concrete surface was measured by three concentrically placed linear voltage displacement transducers (LVDTs) secured to the bar by means of a metal collar as shown in Figure 2.2. LVDTs were placed 120º apart in the horizontal plane, and displacement readings were averaged to account for any eccentricities. After reaching the slip of 14 mm at the loaded end, all the instrumentation was removed from the bar and it was completely pulled from the concrete for inspection.

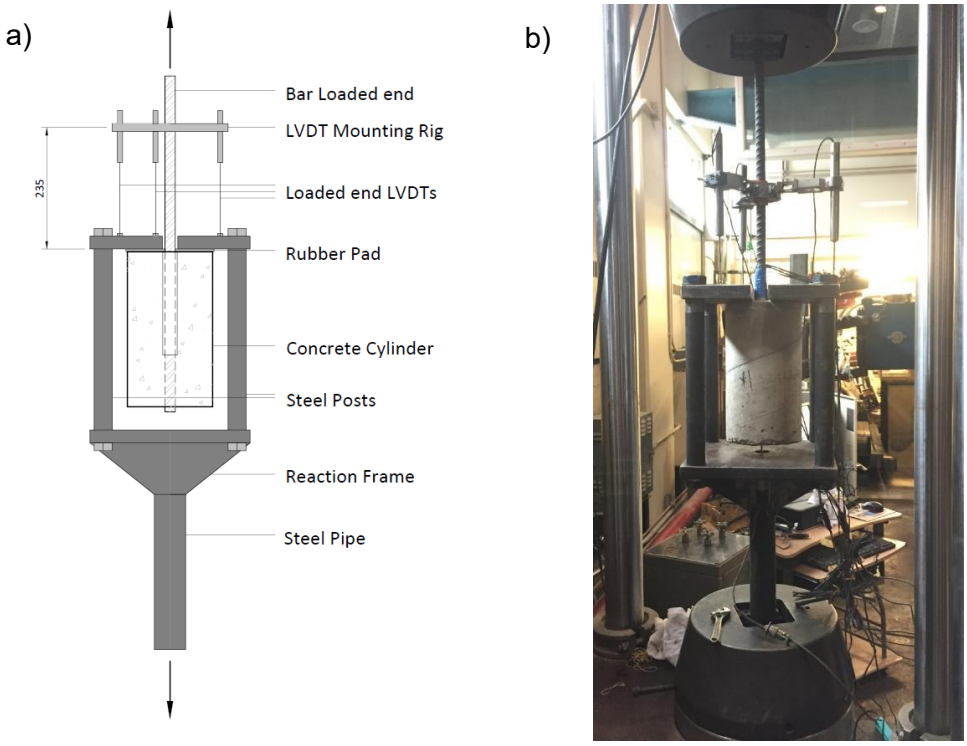

Figure 2.2: a) Schematic and b) actual view of the pull-out test setup

3. RESULTS AND DISCUSSION

3.1 Concrete material properties

3.1.1 Unrestrained expansion of reactive and control prisms

Extent of concrete deterioration due to ASR was quantified based on the unrestrained longitudinal expansion of standardized prisms monitored on a regular basis. It should be noted that prior to specimen conditioning inside the environmental chamber both control and reactive prisms had undergone a moderate amount of shrinkage. Control concrete shrank by around 0.12%, while reactive by 0.13% on average. Since these quantities are almost equal, it was concluded that no ASR expansion had taken place during the specimens storage in the ambient lab enviroment of 25°C and 65% RH and reactive mix behaved as a nonreactive concrete.

After the onset of curing in the chamber, reactive prisms started exhibiting signs of expansion typical for ASR concrete. Free concrete expansion as a function of conditioning period is depicted in Figure 3.1 for both ASR and REG concretes. Destructive testing of concrete specimens took place at three distinct specimen test ages:

- Phase 0 tests commenced after 23 days of accelerated curing with the minimal level of ASR concrete free expansion (close to 0.020%);
- Phase 1 tests were conducted after 132 days (4.5 months) of conditioning with the ASR prisms' expansion of about 0.072%;
- Phase 2 tests were performed after 212 days (7 months) of curing inside the chamber after free expansion levelled off at 0.121%.

Also note that after around 100 days of accelerated curing, ASR prisms' expansion started to plateau at a level of 0.070%. As the anticipated amount of free expansion was somewhat higher, it was assumed that the steam was only moderately effective in accelerating ASR. Hence, it was decided to outfit the environmental facility with the ceiling sprinklers along its perimeter to saturate the chamber with moisture in addition to steam. Sprinklers were introduced when all the specimens had sustained 147 days of curing (marked with a vertical green line in Figure 3.1). Sprinklers proved to be successful in accelerating ASR, and roughly 50 days after their installation concrete expansion started plateauing at the level of

about 0.121%. It was concluded that the expansive potential of the reactive mix had reached exhaustion at this age, which corresponded to the commencement of Phase 2 tests.

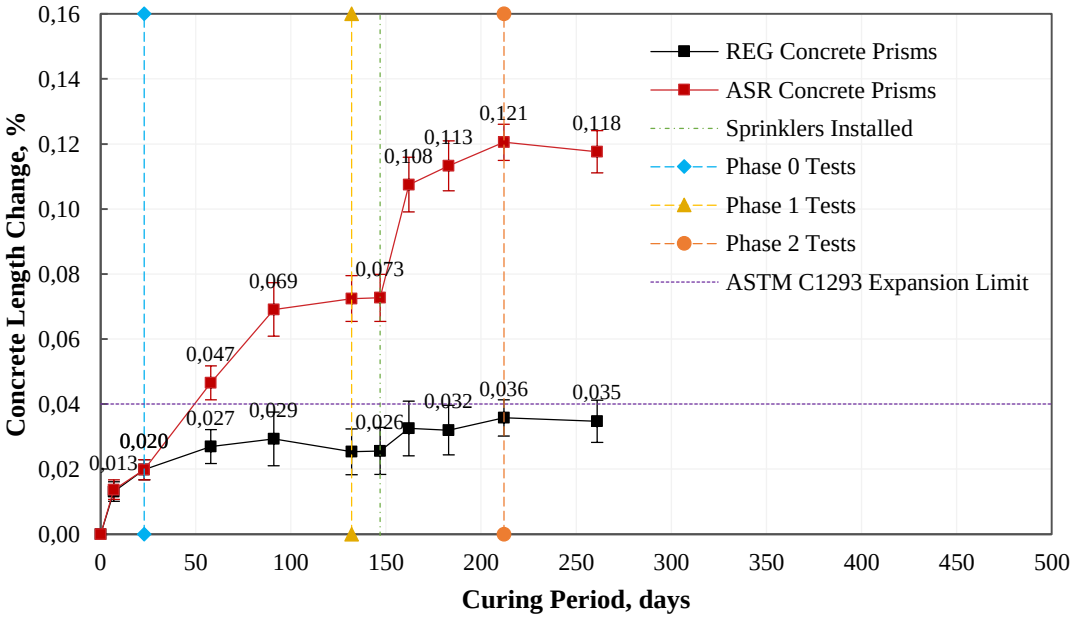

Figure 3.1: Free expansion of reactive and control concrete prisms along with the experimental timeline

3.1.2 Mechanical properties

Concrete compressive strength and modulus of elasticity of ASR and REG concretes were determined at 28 days after casting and after 23 (Phase 0), 132 (Phase 1) and 212 (Phase 2) days of accelerated curing. Additionally, a few cylinders were also tested after 261 days of chamber storage; this test period is referred to as Phase 3. Each response curve and strength and stiffness values represent average of six cylinder tests.

Table 3.1: Reactive and control concrete material properties

Testing Period	Curing Period, days	Value (mean ± standard deviation)					
		Control Concrete			Reactive Concrete		
		Age since Casting, days	f'_c (MPa)	E_{cs} (GPa)	Age since Casting, days	f'_c (MPa)	E_{cs} (GPa)
28 days	0	28	47.4±1.60	30.6±1.22	28	36.2±0.98	28.7±1.52
Phase 0	23	402	47.3±1.25	29.3±1.34	367	39.6±1.59	26.6±1.16
Phase 1	132	511	53.8±1.61	34.9±2.01	476	53.4±2.45	25.7±1.92
Phase 2	212	591	59.9±2.58	34.3±2.38	556	51.9±1.61	23.4±0.74
Phase 3	261	640	63.0±1.92	33.7±0.61	605	54.6±1.48	24.7±1.66

Concrete strength and stiffness data are summarized in Table 3.1. Average stress-strain relationships are shown in Figure 3.2(a) and (b) for REG and ASR cylinders, respectively. As illustrated in these graphs, there was no noticeable change between the 28-day strength and the peak stress measured after 23 days of accelerated curing (i.e. Phase 0) for both concrete types. A lack of strength increase between 28 days and 367-402 days is expected considering that the lab conditions with the 65% RH would slow the hydration process and cause shrinkage of conrete. However, an increase in strength was observed between Phase 0 and Phase 1. Although this increase was rather moderate for REG concrete (14% of the 28-day result), ASR concrete strength was enhanced by 48%. Such compressive

strength growth of ASR affected concrete containing Spratt aggregates has been reported by other researchers [22, 23]. Most likely, this strength enhancement of ASR concrete is attributed to the slow reactivity of some aggregates coupled with the continuous hydration of the cement constituent of concrete. After the initial increase in f_c', the steady state was reached in the ASR concrete behavior, and it ceased to exhibit any significant changes in its compressive strength (Figure 3.2(b)). On the other hand, REG concrete was continuously gaining strength over time, albeit at a lower rate than between Phases 0 and 1 (Figure 3.2(a)).

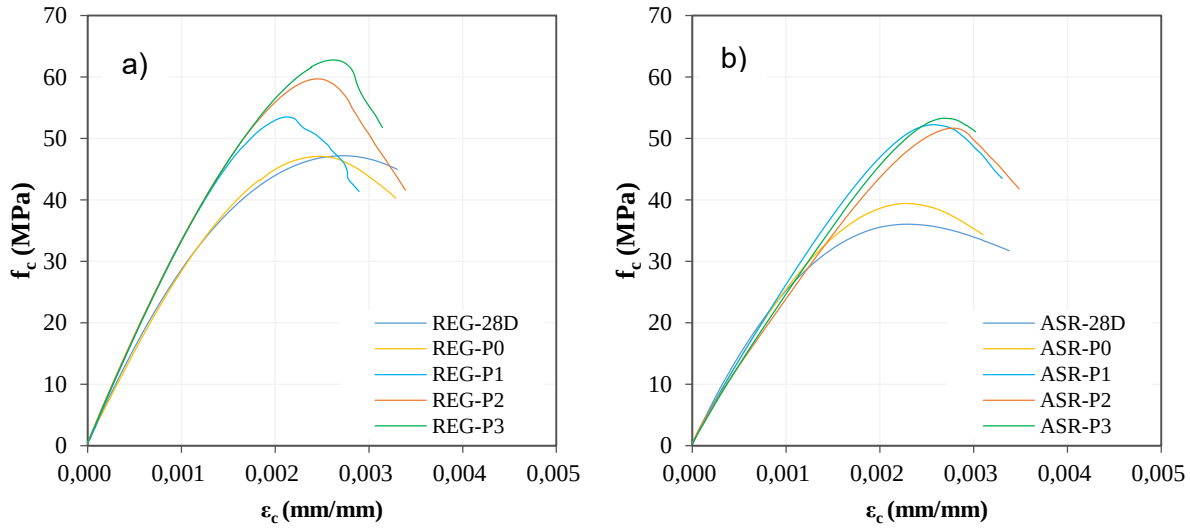

Figure 3.2: Comparison of a) control and b) reactive concrete average stress-strain response

Similar to f_c', secant elastic modulus of REG concrete increased between testing Phase 0 and Phase 1; no appreciable changes in concrete stiffness were observed from that point onward. On the contrary, the ASR concrete experienced a systematic reduction in its secant modulus following Phase 0 tests. The highest loss of 19% was determined after 7 months (Phase 2) of accelerated curing relative to the 28-day stiffness (Table 3.1).

3.2 Pull-out tests

3.2.1 Experimental results

The average nominal bond stress was calculated by diving the applied load by the bar surface area along the lenght of embedment. Since concrete of different ages, strengths and compositions (ASR and REG) was tested during Phases 0, 1 and 2, its mechanical properties varied. Thus, to evaluate bond strength at different concrete ages, peak bond stresses determined in Phases 1 and 2 tests of each type of concrete were normalized with respect to the square root of the average f_c' as measured at Phase 0 for the same concrete mix. REG concrete Phase 0 average batch strength $f_{c\,norm}'$ was 47.3 MPa, while for ASR concrete it was 39.6 MPa as was reported in Table 3.1. Lastly, averaged LVDT readings at the loaded bar end were adjusted by the bar elastic elongation between the point of LVDT attachment to the rebar and concrete surface (i.e. distance of 235 mm, Figure 2.2(a)).

Table 3.2 and Table 3.3 present test results obtained from the pull-out testing of REG and ASR specimens, respectively, for the three test phases. Specimens were designated in the following manner: **WWW-YY-PX-SZ,** where WWW refers to the concrete type (ASR or REG), YY shows presence or absence of reinforcement (NR or TRLN specimen group), PX indicates testing phase (P0, P1 or P2), and SZ represents specimen replicate number (S1, S2 or S3). Also, PO denotes the pull-out frictional failure type.

Post-test inspection of the sliced specimens revealed that the actual bonded lengths in specimens, REG-NR-P0-S1 and REG-TRLN-P0-S1 were smaller than designed. This was accounted for in the peak bond stress calculations. Additionally, results from specimens ASR-NR-P2-S3 and ASR-TRLN-P0-S1 were not incorporated in the analysis as they failed prematurely due to the poor concrete compaction along the length of embedment.

Since the reactive prisms showed no expansion prior to the concrete conditioning, it was concluded that the pull-out specimens had also not been affected by ASR during this period. Therefore, any ASR related expansion had only taken place after the onset of curing and no adjustments to the bond stress and strength results are needed to account for any pre-conditioning ASR development.

Table 3.2: Control concrete pull-out test results

Specimen ID	f'_c (MPa)	$f'_{c\,norm}$ (MPa)	Peak Bond Stress (MPa)	Normalized Peak Bond Stress (MPa)	Loaded end slip (mm)	Failure Type
REG-NR-P0-S1	48.2	47.3	9.45	9.36	2.15	PO
REG-NR-P0-S2			14.35	14.21	2.26	PO
REG-NR-P0-S3			10.53	10.43	2.03	PO
REG-NR-P1-S1	55.0		11.14	10.33	1.24	PO
REG-NR-P1-S2			12.39	11.48	1.52	PO
REG-NR-P1-S3			12.93	11.99	1.54	PO
REG-NR-P2-S1	62.0		15.59	13.61	1.91	PO
REG-NR-P2-S2			11.44	9.99	1.54	PO
REG-NR-P2-S3			14.09	12.31	1.83	PO
REG-TRLN-P0-1	46.4		17.58	17.75	1.48	PO
REG-TRLN-P0-2			14.84	14.98	1.15	PO
REG-TRLN-P0-3			15.62	15.78	1.45	PO
REG-TRLN-P1-S1	52.6		16.32	15.48	1.63	PO
REG-TRLN-P1-S2			18.73	17.76	1.61	PO
REG-TRLN-P1-S3			14.48	13.74	1.06	PO
REG-TRLN-P2-S1	57.8		20.36	18.42	1.40	PO
REG-TRLN-P2-S2			17.12	15.49	1.36	PO
REG-TRLN-P2-S3			15.20	13.75	1.21	PO

Table 3.3: Reactive concrete pull-out test results

Specimen ID	f'_c (MPa)	$f'_{c\,norm}$ (MPa)	Peak Bond Stress (MPa)	Normalized Peak Bond Stress (MPa)	Loaded end slip (mm)	Failure Type
ASR-NR-P0-S1	40.5	39.6	11.52	11.40	1.96	PO
ASR-NR-P0-S2			10.62	10.50	3.16	PO
ASR-NR-P0-S3			13.86	13.71	2.44	PO
ASR-NR-P1-S1	54.9		11.63	9.88	1.78	PO
ASR-NR-P1-S2			13.23	11.24	1.52	PO
ASR-NR-P1-S3			10.28	8.74	1.53	PO
ASR-NR-P2-S1	52.7		10.86	9.42	1.30	PO
ASR-NR-P2-S2			11.09	9.62	1.67	PO
ASR-TRLN-P0-2	38.7		13.28	13.44	1.49	PO
ASR-TRLN-P0-3			12.62	12.76	1.35	PO
ASR-TRLN-P1-S1	52.0		15.05	13.15	2.10	PO
ASR-TRLN-P1-S2			13.41	11.72	2.83	PO
ASR-TRLN-P1-S3			15.30	13.37	1.08	PO
ASR-TRLN-P2-S1	51.1		18.28	16.10	1.53	PO
ASR-TRLN-P2-S2			14.76	13.00	2.88	PO
ASR-TRLN-P2-S3			13.73	12.09	2.35	PO

3.2.2 Bond stress-slip response

Figure 3.3(a) and (b) compare the representative bond responses of the plain and reinforced pull-out specimens, respectively. In general, all the specimens exhibited a classical stress-slip responses and bond frictional pull-out failure patterns, irrespective of concrete type and degree of confinement. The ascending branch was characterized by a rapid change in the average bond stress while the bar displacement relative to concrete (i.e. slip) remained quite small (less than 2 mm). Beyond the peak load, a gradual decay in bond resistance was observed with the increasing slip. When concrete got fully sheared off by the bar indentations and mechanical interlock ceased to be engaged, bond response plateaued and became independent of slip. The only bond mechanism remaining between the two materials was that of friction.

In Figure 3.3(a) not much difference can be noted in the pre-peak and post-peak bond responses of the NR specimens, regardless of the testing phase and concrete mix. Similar conclusion can be made about the TRLN cylinders' behavior in Figure 3.3(b), although, the post-peak stiffness of both REG and ASR specimens shows greater variability compared to the NR graphs. However, what is notable is the bond behavior immediately after the peak of the TRLN group. While bond resistance of REG cylinders dropped rapidly after reaching the ultimate strength (note the spikes in the REG concrete stress-slip curves of Figure 3.3(b)), especially at later testing phases, maximum average bond stress had a tendency to plateau up to the slip of around 4 mm in the ASR TRLN group. Thus, slippages of these specimens at maximum bond stresses were much greater compared to the REG mix (Table 3.2 and Table 3.3). Such deviation in the bond-slip response of the ASR TRLN specimens points to the enhanced confinement provided by the transverse reinforcement potentially resulting from the expansion of ASR concrete.

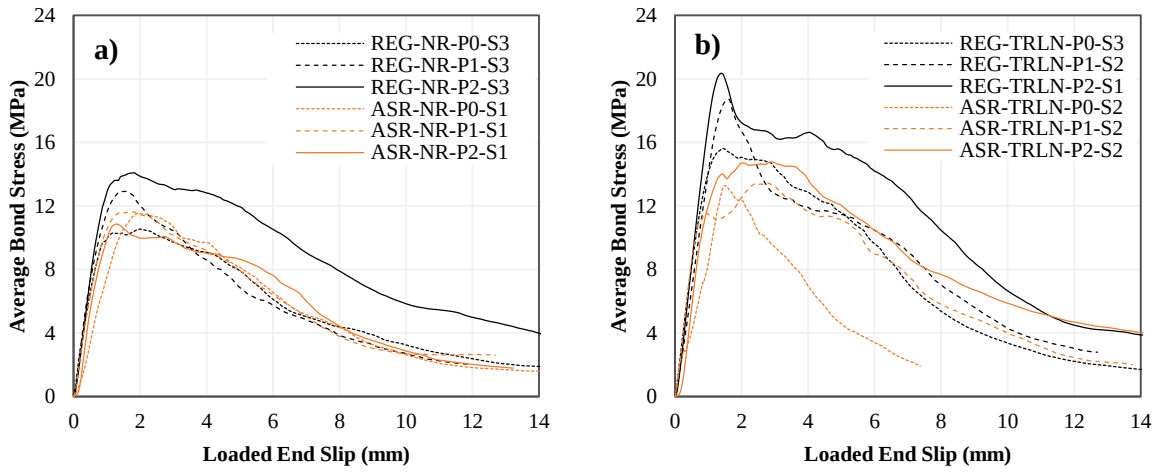

Figure 3.3: Comparison between the a) un-reinforced and b) reinforced concrete behaviour

3.2.3 Bond strength

Figure 3.4(a) summarizes average bond strength test results for control NR and TRLN cylinders. It shows a consistent increase in the peak bond stresses between test Phases 0 and 2, for both types of specimens. This behavior is primarily attributed to the enhancement in concrete compressive strength with age as moist conditions inside the chamber were conducive to continuously promoting the hydration reaction. To eliminate the effect of f_c' on bond resistance, bond strength at different test ages was normalized with respect to the average concrete compressive strength at Phase 0 and the results are depicted in Figure 3.4(b). It can be noted that after the normalization no appreciable difference in bond strength data was observed between different testing phases within the same concrete reinforcement configuration. This indicates that the bond resistance of control concrete was increasing proportionally to $\sqrt{f_c'}$ and was not affected by any other variables.

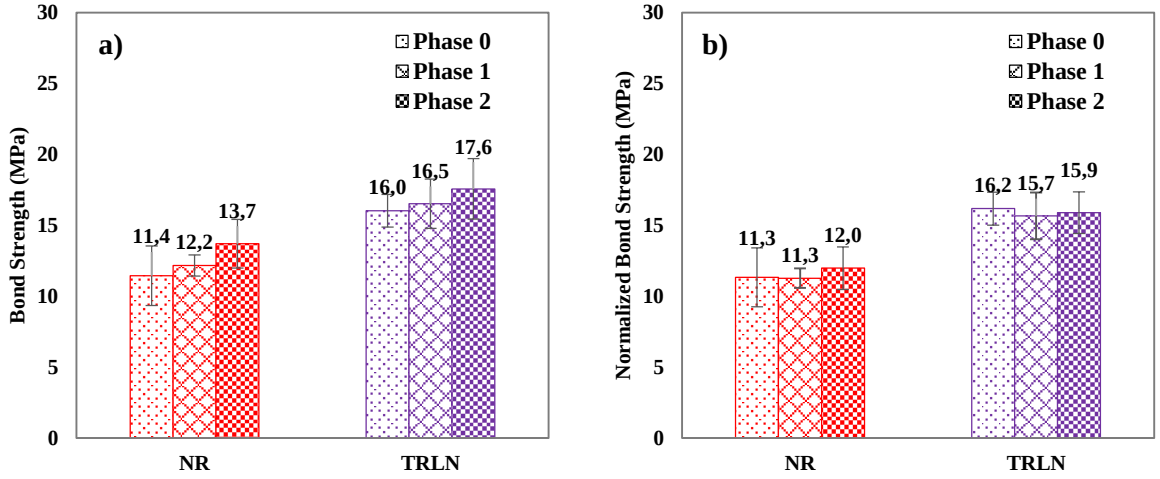

Figure 3.4: Bond strength of control concrete: a) actual and b) normalized results

Similarly, actual and normalized peak bond strength data for ASR concrete is compared in Figure 3.5(a) and (b), respectively. As illustrated in Figure 3.5(a), despite the fact that the average concrete compressive strength of ASR concrete increased from 39.6 MPa to 51.9 MPa between Phase 0 and 2 (Table 3.1), no appreciable changes in bond strength were observed in the unreinforced (NR) specimens between these time intervals. As a result, the normalized data from Figure 3.5(b) shows that the unconfined concrete (NR) experienced a 20% reduction in bond strength during this period. For reinforced specimens (TRLN group), normalized bond strength results in Figure 3.5(b) show that no reduction in bond capacity has taken place over the three testing ages. This implies that the enhancement in bond resistance of the TRLN specimens depicted in Figure 3.5(a) (actual results) was almost proportional to the change in $\sqrt{f_c'}$, as was also the case in the REG concrete response (Figure 3.4(a)). It can be concluded that the presence of transverse reinforcement in the TRLN cylinders was beneficial in confining the concrete core after cover cracking due to ASR. It prevented the loss of bond strength in the confined specimens, unlike in the ASR NR specimens, where concrete cover cracking had weakened the bond resistance. Extent of surface cracking in the reactive NR and TRLN specimens after 212 days of conditioning (i.e. Phase 2) can be seen in Figure 3.6(a) and (b), respectively.

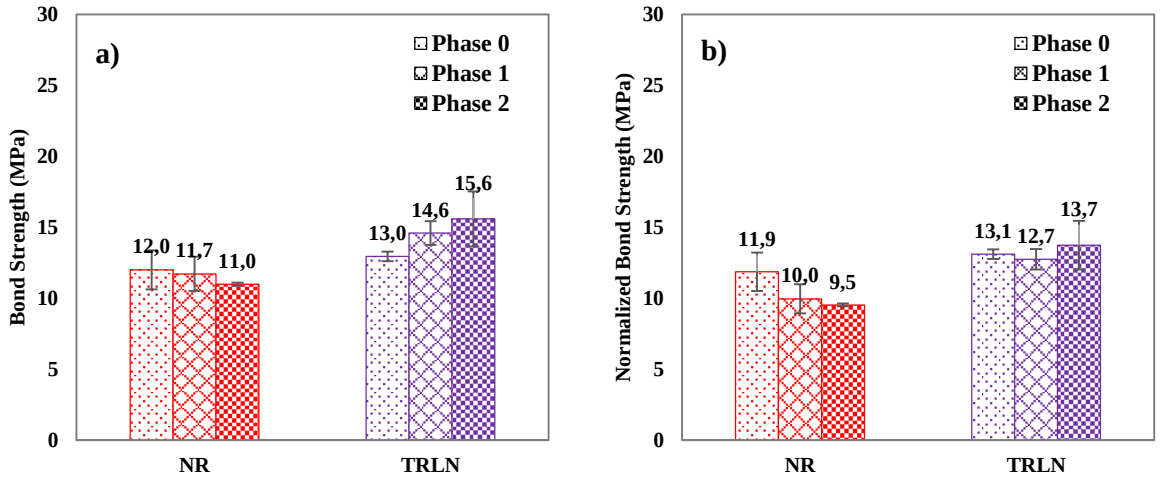

Figure 3.5: Bond strength of reactive concrete: a) actual and b) normalized results

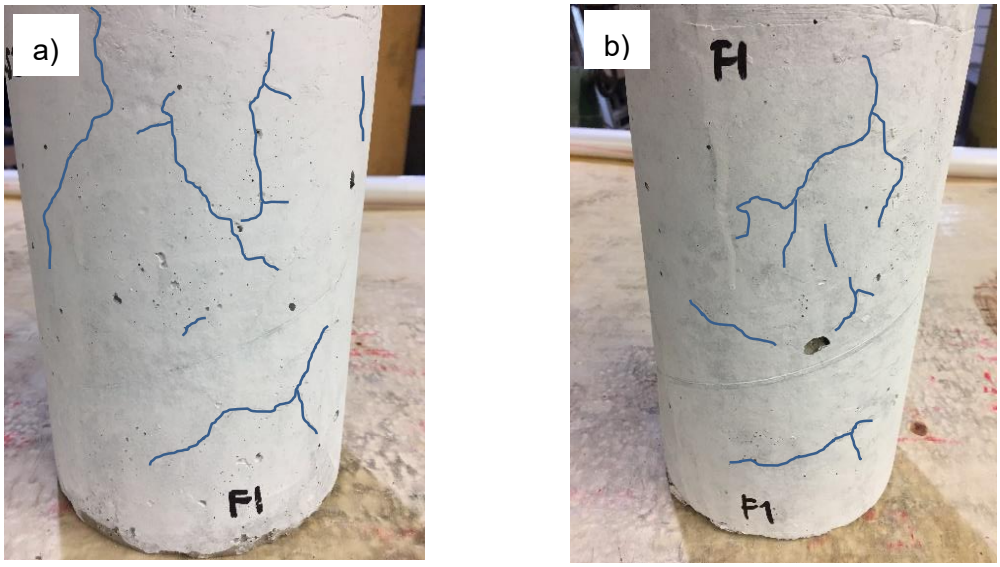

Figure 3.6: Surface cracking in the reactive a) NR and b) TRLN specimens after 212 days of accelerated curing (corresponding to Phase 2 tests)

4. CONCLUSIONS

Based on the work reported herein, the following conclusions can be made:

1. Reactive concrete expanded significantly less (~0.12%) than anticipated. Reduced expansion can perhaps be attributed to the advanced concrete age at the onset of hot and humid conditioning regime (379 days for REG specimens and 344 for ASR). No expansion was recorded in the reactive concrete prisms prior to conditioning.
2. ASR and associated cracking did not have a severe detrimental effect on the reactive concrete compressive strength; concrete managed to gain strength over time (~51% beyond 28 days). However, as ASR evolved, modulus of elasticity of the reactive concrete dropped by 19% compared to the 28-day value.
3. Conventional shape of the bond-slip response of reactive concrete was not altered by the alkali-silica reaction.
4. As expected, reinforced specimens generally displayed higher bond resistance due to the confining effects of the transverse reinforcement. This behaviour was consistent between both reactive (ASR) and control (REG) specimens.
5. Based on the normalized strength results, unreinforced (NR) reactive (ASR) specimens experienced a 20% reduction in bond strength after a 7-month long exposure to high temperature and high humidity environment. Normalized peak bond data has also shown that no loss in bond capacity occurred in the TRLN cylinders as a result of ASR. This behavior was similar to that of the TRLN specimens made from the control (REG) concrete.

5. ACKNOWLEDGEMENTS

The authors acknowledge the funding provided through a contract by Canadian Nuclear Safety Commission (CNSC). This paper does not represent or express the technical position of CNSC on the subject. Appreciation is also due to the technical staff of the Structural Laboratories at the University of Toronto for their assistance with various aspects of this project.

6. REFERENCES

[1] Hobbs DW (1988) Alkali-silica reaction in concrete. Thomas Telford, London

[2] Swamy RN (1992) The alkali-silica reaction in concrete. Blackie and Son Ltd, Glasgow and London

[3] Rogers C, Grattan-Bellew PE, Hooton RD, et al (2000) Alkali – aggregate reactions in Ontario. Can J Civ Eng 27:246-260

[4] Swamy RN, Al-Asali MM (1988) Engineering properties of concrete affected by alkali-silica reaction. ACI Mater J 85:367-374. https://doi.org/10.14359/2288

[5] Ahmed T, Burley E, Rigden S, Abu-Tair A (2003) The effect of alkali reactivity on the mechanical properties of concrete. Constr Build Mater 17:123-144

[6] Giaccio G, Zerbino R, Ponce JM, Batic OR (2008) Mechanical behavior of concretes damaged by alkali-silica reaction. Cement and Concrete Research 38:993-1004. https://doi.org/10.1016/j.cemconres.2008.02.009

[7] Marzouk H, Langdon S (2003) The effect of alkali-aggregate reactivity on the mechanical properties of high and normal strength concrete. Cem Concr Compos 25:549-556. https://doi.org/10.1016/S0958-9465(02)00094-X

[8] Koyanagi W, Rokugo K, Ishida H (1986) Failure behaviour of reinforced concrete beams deteriorated by alkali-silica reactions. In: Proceedings of the 7th International Conference on Concrete Alkali-Aggregate Reactions. Noyes Publications, New Jersey, pp 141-145

[9] Inoue S, Fujii M, Kobayashi K, Nakano K (1989) Structural behaviour of reinforced concrete beams affected by alkali-silica reaction. In: Proceedings of the 8th International Conference on Alkali-Aggregate Reactions. Taylor&Francis, Kyoto, pp 727-732

[10] Ahmed T, Burley E, Rigden S (1998) The static and fatigue strength of reinforced concrete beams affected by alkali-silica reaction. ACI Mater J 95:356-368. https://doi.org/10.14359/380

[11] Deschenes D, Bayrak O, Folliard K (2009) ASR/DEF – Damaged bent caps: Shear tests and field implications (Technical report No. 12-8XXIA006). Austin, TX

[12] Bracci JM, Gardoni P, Eck MK, Trejo D (2012) Performance of lap splices in large-scale column specimens affected by ASR and/or DEF (Report FHWA/TX-12/0-5722-1). Austin, TX

[13] Giannini E, Folliard K, Zhu J, et al (2013) Non-destructive evaluation of in-service concrete structures affected by alkali-silica reaction (ASR) or delayed ettringite formation (DEF) – Final report, Part I (FHWA/TX-13/0-6491-1). Austin, TX

[14] Barbosa RA, Hansen SG, Hoang LC, Hansen KK (2018) Residual shear strength of a severely ASR-damaged flat slab bridge. Engineering Structures 161:82-95. https://doi.org/10.1016/j.engstruct.2018.01.056

[15] Chana PS (1989) Bond strength of reinforcement in concrete affected by alkali silica reaction (Contractor Report 141). Crowthorne, UK

[16] Clark LA (1989) A critical review of the structural implications of the alkali-silica reaction in concrete (Contractor report 169). Crowthorne, UK

[17] Haddad RH, Numayr KS (2007) Effect of alkali-silica reaction and freezing and thawing action on concrete-steel bond. Construction and Building Materials 21:428-435. https://doi.org/10.1016/j.conbuildmat.2005.07.012

[18] Zhychkovska O (2020) Effect of alkali-silica reaction (ASR) on steel-concrete bond. Master's Thesis, University of Toronto

[19] ASTM C1293 (2015) Standard test method for determination of length change of concrete due to alkali-silica reaction. ASTM International, West Conshohocken, PA

[20] Gautam BP, Panesar DK, Sheikh SA, Vecchio FJ (2017) Effect of coarse aggregate grading on the ASR expansion and damage of concrete. Cement and Concrete Research 95:75-83. https://doi.org/10.1016/j.cemconres.2017.02.022

[21] ASTM C1260 (2014) Standard test method for potential alkali reactivity of aggregates (Mortar-bar method). ASTM International, West Conshohocken, PA

[22] Monette LJ, Gardner NJ, Grattan-Bellew PE (2002) Residual strength of reinforced concrete beams damaged by alkali-silica reaction – Examination of damage rating index method. ACI Mater J 99:42-50. https://doi.org/10.14359/11315

[23] Gautam BP (2016) Multiaxially loaded concrete undergoing alkali-silica reaction (ASR). PhD Thesis, University of Toronto